Journal of Cellular Biochemistry 103:136–148 (2008)

Intranuclear Mobility of Estrogen Receptor α and Progesterone Receptors in Association With Nuclear Matrix Dynamics

KenIchi Matsuda,* Mayumi Nishi, Hisamitsu Takaya, Natsuko Kaku, and Mitsuhiro Kawata

Department of Anatomy and Neurobiology, Kyoto Prefectural University of Medicine, Kawaramachi Hirokoji, Kamigyo-ku, Kyoto 602-8566, Japan

Abstract We analyzed the intranuclear dynamics of estrogen receptor α (ERα) and progesterone receptor (PR)-A/B labeled with different spectral variants of green fluorescent protein (GFP) in living cells. The distribution of ERα and PR-A/B were changed from a diffuse to discrete pattern after the addition of both ligands, but the extent of discrete cluster formation of PR-A/B was lower than that of ERα. The nuclear areas where PR-A/B were accumulated were colocalized with the cluster of ERα, suggesting that cross-talk in the transcriptional regulation occurred in the loci. Fluorescence recovery after photobleaching (FRAP) analysis revealed that the mobility of PR-A/B was hastened by the coexistence of ERα, while the mobility of ERα was not changed by the coexistence of PR-A/B. Cluster formation was correlated with the nuclear matrix binding, because nuclear matrix binding capacity was also lower in PR-A/B than ERα. By ATP-depletion from the cells, most of ERα and PR-A/B were bound to the nuclear matrix and their mobilities were extinguished both in the absence and presence of ligand. Fluorescent protein (FP) tagged nuclear matrix component protein (NuMA), which was colocalized with ERα and PR-A/B, showed ATP-dependent rapid exchange in the nucleus. These results indicate that the mobility of ERα and PR-A/B is associated with the dynamics of the nuclear matrix. J. Cell. Biochem. 103: 136–148, 2008.

Key words: estrogen receptor; progesterone receptor; FRAP; nuclear matrix; NuMA; ATP; GFP

Estrogen and progesterone regulate various physiological functions, such as ovarian action, growth and differentiation of the uterine endometrium and mammary glands, and gonadotropin-releasing hormone secretion and sexual behavior control in the brain [Kawata et al., 1998]. Specific receptors for estrogen and progesterone are members of the nuclear receptor superfamily of ligand-dependent transcription factors [Kawata et al., 1998]. To date, two estrogen receptors (ERα and ERβ) have been identified that are encoded by different genes [Greene et al., 1986; Kuiper et al., 1996]. ERα and ERβ have been considered to positively or negatively regulate transcription of target genes by forming homo- or heterodimers [Cowley et al., 1997; Pace et al., 1997]. The progesterone receptor also exists as two isoforms (PR-A and PR-B) [Kastner et al., 1990]. They are encoded by the same gene and differ only in that PR-B contains an additional 164 amino acids at the amino terminus of PR-A. It has been reported that there are differences between PR-A and -B in response to agonists and antagonists and in cell- and promoter-dependent activity [Vegeto et al., 1993; Giangrande et al., 2000; Richer et al., 2002]. It has been well known that ERα and PRs are coexpressed in the same cells in several areas of the target tissues [Lau et al., 1999; Jarvinen et al., 2000; Greco et al., 2001]. In addition, a number of reports demonstrated that ERα and PRs had synergistic or inhibitory cross-talk in their transcriptional regulation in promoter type- and PR subtype-specific manners [Cato and Ponta, 1989; Meyer et al., 1989; Wen et al., 1994; Kraus et al., 1995].

Grant sponsor: The Ministry of Education, Science, Sports, Culture and Technology, Japan.

*Correspondence to: KenIchi Matsuda, Department of Anatomy and Neurobiology, Kyoto Prefectural University of Medicine, Kawaramachi Hirokoji, Kamigyo-ku, Kyoto 602-8566, Japan. E-mail: matsuken@koto.kpu-m.ac.jp

Received 23 February 2007; Accepted 2 April 2007

DOI 10.1002/jcb.21393

Live cell imaging techniques using green fluorescent protein (GFP) fusion protein revealed intracellular trafficking and intranuclear dynamics of the ovarian steroid hormone receptors and their coactivator [Kawata et al., 2001]. GFP labeled PR-A and -B (GFP-PR-A and -B) were differentially localized between the nuclear and cytoplasmic compartments in an unliganded state. GFP-PRA was predominantly located in the nucleus; whereas, GFP-PRB distributed between the cytoplasmic and nuclear compartments. In the presence of ligand, GFP-PR-A and -B were localized in the nucleus completely [Lim et al., 1999]. GFP-tagged ERα and ERβ (GFP-ERα and -ERβ) were diffusely distributed throughout the nucleoplasm in the absence of ligand. Upon the addition of ligand, a redistribution of GFP-ERα and -ERβ from a diffuse to discrete pattern occurs within 10 min [Htun et al., 1999; Matsuda et al., 2002]. The discrete clusters of ERα are associated with steroid receptor coactivator-1 (SRC-1) and a chromatin remodeling protein, BRG-1 [Stenoien et al., 2000; Matsuda et al., 2002], suggesting that clusters of ERs are involved in the transcriptional regulation through structural changes of chromatin. Recent fluorescence recovery after photobleaching (FRAP) technique showed that ligand-activated ERα was highly mobile within the nucleus. It has been proposed that the rapid mobility of the steroid hormone receptors depends on ATP, proteasome activity, and chaperone/cochaperone functions [Stenoien et al., 2001; Elbi et al., 2004].

The nuclear matrix is a filamentous protein meshwork and is thought to be involved in organization of chromosomes and the regulation of DNA transcription and replication within the nucleus. The nuclear mitotic apparatus protein (NuMA), first identified as a protein localizing on the spindle poles of mitotic cells, is a component of the nuclear matrix in interphase cells [Zeng et al., 1994; Harborth et al., 1999; Gribbon et al., 2002]. It has long been understood that steroid receptors associate with the nuclear matrix ligand-dependently [Hora et al., 1986; Barrack, 1987; Hu et al., 1994; Tang and DeFranco, 1996], and thus hypothesized that the nuclear matrix binding may play an important role in the regulation of steroid hormone receptor-mediated transcription. In the previous study, Stenoien et al. [2000] visualized a nuclear matrix binding property of ERα using GFP-ERα, and showed that most of ligand-activated GFP-ERα was associated with the nuclear matrix by forming discrete clusters. In addition, SRC-1 also associated with nuclear matrix at the clusters of ligand-activated GFP-ERα.

In the present study, we investigated the change of intranuclear distribution and mobility of ERα and two PR isoforms in response to ligands in living cells by tagging the receptors with different spectral variants of GFP, yellow fluorescent protein (YFP) and cyan fluorescent protein (CFP). Using these fluorescent protein (FP) chimera receptors, we characterized the nuclear matrix binding manner of ERα and PR-A/B. In addition, by coexpressing FP-ERα/PRs with FP-labeled NuMA, the correlation between the mobility of the receptors and nuclear matrix dynamics was examined.

MATERIALS AND METHODS

Plasmid Construction

To create the Y/CFP-PR-B and Y/CFP-PR-A construct, a BglII site was introduced just upstream of the 1st ATG and the 2nd ATG of the rat PR genes (pratPR6B, provided by Dr. B. Katzenellenbogen, Department of Molecular and Integrative Physiology, University of Illinois, Urbana, IL) [Kastner et al., 1990], respectively, with a QuikChange Site-Directed Mutagenesis Kit (Stratagene, La Jolla, CA). After cutting with BglII and HincII, the gene was then subcloned in-frame into pEY/CFP-C1 vectors (BD Biosciences Clontech, Mountain View, CA) cut with BglII and SmaI. Details of the Y/CFP-ERα construct have been published elsewhere [Matsuda et al., 2002]. The expression plasmid of the NuMA-GFP was provided by Dr. D.A. Compton, Department of Biochemistry, Dartmouth Medical School, Hanover, NH [Kisurina-Evgenieva et al., 2004]. To generate the NuMA-YFP construct, NuMA cDNA was digested from the NuMA-GFP plasmid with BglII and EcoRI and then ligated to the pEYFP-N1 vector (BD Biosciences Clontech) cut with the same restriction enzymes.

Cell Culture and Transfection

COS-1 cells and HeLa cells were maintained in a humidified atmosphere at 37°C with 5% CO_2/95% air in DMEM (Invitrogen, Carlsbad, CA), without phenol red, supplemented with

10% FCS. On the day before transfection, cells were reseeded in a 4-well multidish with 16-mm diameter (Nunc, Roskilde, Denmark) at an initial plating density of 2×10^4 cells per well in 400 μl of medium for fluorescence microscope imaging, and on a 10 mm diameter glass base precoated with poly-L-lysine of 35 mm glass-bottomed dish (Matsunami, Tokyo, Japan) at an initial plating density of 1×10^4 cells per dish in 200 μl of medium for confocal laser scan imaging. Plasmid DNA (250 ng) was transiently transfected into cells with a liposome-mediated method using LipofectAMINE PLUS (Invitrogen) according to the manufacturer's instructions. Before analyzing, the cells were washed three times with 400 or 2,000 μl of PBS, and then cultured again in 400 or 2,000 μl of a serum free medium, OPTI MEM (Invitrogen), respectively, for at least 15 h to remove any effects of the remaining steroid hormones. We treated the cells with 17β-estradiol (E2) at a final concentration 10^{-8} M and progesterone (P) at a final concentration 10^{-7} M throughout this study. ATP-depletion experiment [Hu et al., 1994; Tang and DeFranco, 1996] was carried out by incubating cells in ATP-depletion medium (glucose-free DMEM (Invitrogen) supplemented with 10 mM sodium azide and 6 mM deoxyglucose) for 60 min. To inhibit proteasome activity, cells were treated with 10 μM MG132 for 5 h. The effect of MG132 was confirmed by the inhibition of intranuclear mobility of CFP-ERα and CFP-PR-A/B [Stenoien et al., 2001].

Transcriptional Assays

COS-1 cells (3×10^5) plated on 35-mm dishes were cotransfected with 1 μg of pMMTV-Luc reporter plasmid [Ogawa et al., 1995] and 10 ng of either Y/CFP-PR-A or Y/CFP-PR-B expression plasmids using LipofectAMINE PLUS. pAct-βGal (1μg), a β-actin promoter driven β-galactosidase expression plasmid, was also transfected as an internal standard to estimate the transfection efficiency [Inoue et al., 1999]. Cells were incubated in the absence or presence of P for 30 h, washed with 2 ml of PBS and lysed in a buffer from the luciferase assay system, Pica Gene (Toyo Inki, Tokyo, Japan). Cell lysates were centrifuged at 12,000 rpm for 2 min at 4°C and the luciferase activity of the resultant supernatants was assayed at 25°C according to the manufacturer's protocol for the Pica Gene. The results were normalized with β-galactosidase activity measured using a luminescent β-galactosidase Detection Kit II (BD Biosciences Clontech).

Fluorescence Microscope Imaging

The living cell image acquisition was performed in a temperature-controlled room at 37°C [Matsuda et al., 2002; Ochiai et al., 2004]. Images were acquired using a Quantix high-resolution cooled CCD camera (Photometrics) attached to a microscope (IXL70, Olympus Corp., Tokyo, Japan) equipped with an epifluorescence attachment. Cells were observed with a 40× objective lens (LCP PlanF1). YFP fluorescence was observed using a filter set with an excitation of 500 nm and emission of 545 nm, and a dichroic mirror of 525 nm (Omega Optical, Inc., Brattleboro, VT). The CFP fluorescence was observed using a filter set with an excitation of 440 nm and an emission of 480 nm, and a dichroic mirror of 455 nm (Omega Optical, Inc.). When fluorescence images were captured from the cells coexpressing CFP-ERα and YFP-PR-A/B, we selected the cells showing nearly the same fluorescence intensity of CFP and YFP. Time-lapse image capturing and data evaluation were performed using the image analysis software program, MetaMorph (Universal Imaging Corp., West Chester, PA). For high-resolution analysis, an image deconvolution procedure, "Nearest Neighbor Estimate", was applied to the Z-series focal plane images.

Immunofluorescent Labeling

HeLa cells transfected with CFP-PR-A/B and YFP-ERα expression plasmids were fixed with 4% paraformaldehyde in PBS and the subjected to blocking with 2% BSA in PBS including 0.2% Triton X-100 for 1 h at 25°C. The fixed cells were incubated with goat polyclonal anti-BRG-1 (1:300 dilution, Santa Cruz Biotechnology, Inc., Santa Cruz, CA) or rabbit polyclonal anti-SRC-1 (1:300 dilution, Santa Cruz Biotechnology, Inc.) for 12 h at 4°C. Alexa Fluor 633-linked anti-goat or rabbit IgG second antibody, respectively (1:1000 dilution, Molecular Probes, Inc.), was used for detection.

Confocal Laser Scanning Imaging

Confocal fluorescence imaging was performed with a confocal laser microscope (LSM510META, Carl Zeiss Co., Ltd., Jena, Germany) [Nishi et al., 2004; Ochiai et al., 2004]. Cells were observed with a 63× oil immersion objective lens (Plan-Apochromat).

YFP fluorescence was excited with a 514 nm laser and detected by projecting each image of 10 nm intervals from 511.0 through 564.5 nm using an HFT 458/514 dichroic mirror. The CFP fluorescence was excited with a 458 nm laser and detected by projecting each image at 10 nm intervals from 468.2 through 500.3 nm using an HFT 458/514 dichroic mirror. The Alexa Fluor 633 fluorescence was excited with a 633 nm laser and detected by projecting each image at 10 nm intervals from 649.6 through 799.4 nm using an HFT 488/543/633 dichroic mirror. When fluorescence images were captured from the cells coexpressing CFP-ERα and YFP-PR-A/B, we selected the cells showing nearly the same fluorescence intensity of CFP and YFP. Living cell imaging was performed in a micro incubator (CZI-3, Carl Zeiss Co., Ltd.) maintained in a humidified atmosphere at 37°C with 5% CO_2/95% air and attached on the stage of an inverted fluorescence microscope (Axiovert 200M) built in the confocal microscope.

FRAP analysis. FRAP analysis was performed on the confocal laser scanning microscopy [Ochiai et al., 2004]. Bleach was carried out to the region of interest of a 0.5 μm circle within the nucleus at a wavelength of 488 nm (for GFP), 458 nm (for CFP), or 514 nm (for YFP) at the maximum power of the argon laser for 100 iterations. A single Z-section was imaged before and after the addition of ligand at a minimum time interval. Fluorescence intensities of the region of interest were obtained using LSM software and plotted. The half recovery time (t1/2) was determined as the time after bleaching until the fluorescence intensity was recovered to the mean between the level immediately after bleaching and the level reached a plateau.

Nuclear Matrix Extraction

COS-1 cells were seeded on a 35 mm glass base dish with a grid (grid size 55 μm) (Iwaki glass, Tokyo, Japan), transfected with expression plasmid(s) of CFP-ERα and/or YFP-PR-A/B and treated with E2 and P for 1 h. After capturing the fluorescence images, the position of the cell was recognized by the site within the grid. Cells were gently washed with PBS and then sequentially treated in the following manner [Stenoien et al., 2000]. Soluble proteins were extracted by treatment for 3 min with ice-cold CK buffer (10 mM piperazine-N,N′-bis(2-ethanesulfonic acid), 300 mM sucrose, 100 mM NaCl, 3 mM $MgCl_2$, and 0.5% Triton X-100, pH 6.80) containing a cocktail of protease inhibitors (Nacalai, Kyoto, Japan). After capturing the fluorescence images of the same cell, chromatin was removed by digesting with RNAse-free DNaseI (400 U/ml; Roche Molecular Biochemicals, Indianapolis, IN) in digestion buffer (same as CK but with 50 mM NaCl) containing a cocktail of protease inhibitors for 50 min at 32 C. The DNaseI digestion buffer was removed and replaced with 200 μl of fresh digestion buffer with 0.25 M ammonium sulfate, and the cells were incubated for 5 min at room temperature. The ammonium sulfate was removed and replaced with 200 μl of digestion buffer with 2 M NaCl and the cells were incubated for 5 min at room temperature. After washing twice with digestion buffer, a fluorescence image of the same cell was captured.

RESULTS

Characterization of Fluorescent Protein Labeled ERα, PR-A and -B

We previously reported the colocalization and ligand-dependent discrete distribution of FP labeled ERα and ERβ, which acted as ligand dependent transcriptional factors in living cells [Matsuda et al., 2002]. In this study, we used the same FP-ERα constructs. A cDNA fragment containing from the 1st ATG (for PR-B) or 2nd ATG (for PR-A: N-terminal 164 amino acid deletion of PR-B) to the 3′-UTR region of rat PR gene [Kastner et al., 1990] was ligated in-frame to the 3′-end of ECFP and EYFP of CMV promoter driven expression vectors. The constructs were cotransfected with a PR-responsive reporter plasmid, pMMTV-Luc into COS-1 cells (which lack endogenous PR-A/B). When treated with progesterone (P) (final concentration 1×10^{-8} M) for 30 h, FP-PR-A induced about 4.2 to 4.9-fold activation of the PR-responsive reporter gene; whereas, FP-PR-B underwent about 25.1 to 32.1-fold activation. These activation levels were similar to the previous report by Lim et al. [1999] showing that a GFP fusion chimera of PR-A had a modest effect on MMTV transcription as compared with that of PR-B. Thus, it was confirmed that the receptor chimera proteins used in this study maintained their capacity to function as ligand-dependent transcription factors, regardless of the different FPs.

When expression vectors of YFP-PR-A and CFP-PR-B were transfected into COS-1 cells in the absence of ligand, the fluorescence of YFP-PR-A was restricted to the nucleus of the cells; whereas, the fluorescence of CFP-PR-B was observed both in the nucleus and the cytoplasm and the ratio of nuclear CFP-PR-B to cytoplasmic CFP-PR-B varied among the cells (Fig. 1A). In the presence of ligand, the fluorescence of YFP-PR-A and CFP-PR-B was seen only in the nucleus (Fig. 1A). These distribution patterns of FP-PR-A and -B were consistent with the previous report [Lim et al., 1999], and the coexpression of FP-PR-A and -B did not alter the distribution of each FP-PR-A/B.

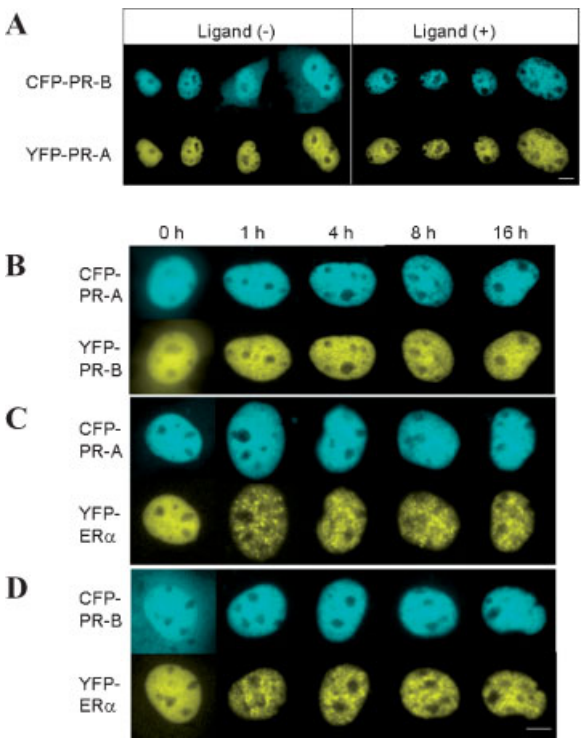

Fig. 1. Subcellular distribution and ligand-dependent intranuclear redistribution of FP-PR-A/B and FP-ERα. COS-1 cells were transiently cotransfected with pCFP-PR-B and pYFP-PR-A, and fluorescent images of randomly selected cells expressing CFP-PR-B and YFP-PR-A at similar level were captured. **A**: Distribution pattern of CFP-PR-B (**upper**) and YFP-PR-A (**lower**) in the same cells cultured in the absence of ligand (**left**) and in the presence of ligand (**right**). **B**: Fluorescent images were captured before and at indicated times after the addition of ligand. COS-1 cells were cotransfected with pCFP-PR-A (**C**) or pCFP-PR-B (**D**) and pYFP-ERα, and fluorescent images were captured before and at the indicated times after the addition of both ligands. All of the images were shown after applying a deconvolution procedure. Bar, 5μm.

Time-Dependent Discrete Distribution of FP-PR-A and -B in Comparison With ERα

We and other group reported that FP-ERα redistribute from a diffuse to discrete pattern in the nucleus within 10 min upon activation with E2 treatment [Stenoien et al., 2000; Matsuda et al., 2002]. We investigated here whether FP-PR-A/B were also redistributed by the addition of P (Fig. 1B). In the absence of ligand, both FP-PR-A and -B showed diffuse distribution. Following the addition of ligand, the distribution of these proteins were changed slightly to discrete at 1 h and reached a maximum at 4 h; however, the extent of discrete cluster formation of CFP-PR-A/B was lower than those of YFP-ERα. The discrete pattern of CFP-PR-A after 4 h was quite similar to that of YFP-PR-B, and these distributions remained the same up to 16 h. The difference of extent of the cluster formation between ERα and PR-A/B was not due to the concentration of ligands, because treatments with either higher (1×10^{-6} M) or lower (1×10^{-8} M) concentration of P did not alter the intranuclear distribution pattern of FP-PR-A/B (data not shown).

To examine the change of discrete cluster formation of ERα and PR-A/B, expression plasmids of CFP-PR-A or CFP-PR-B and YFP-ERα were cotransfected to COS-1 cells (Fig. 1C,D). Before the addition of ligands, the diffuse distribution of CFP-PR-A/B and YFP-ERα in the nucleus was observed. After the addition of both ligands [E2: 1×10^{-8} M, P: 1×10^{-7} M], YFP-ERα showed rapid redistribution to the discrete pattern as single expression, even with the coexistence of activated CFP-PR-A/B. In contrast, the distribution of CFP-PR-A and -B kept more uniform until 16 h after the addition of the hormones than that of YFP-ERα. However, the nuclear areas where CFP-PR-A/B was relatively accumulated were overlapped with clusters of YFP-ERα. This colocalization of CFP-PR-A/B and YFP-ERα was depending on the presence of both ligands, since the overlapped clusters were not observed in the nucleus of the cells treated with either E2 or P (data not shown).

Colocalization of BRG-1 and SRC-1 With the Clusters of FP-PR-A/B and FP-ERα

Colocalization of BRG-1 and SRC-1 with the clusters of FP-PR-A/B and FP-ERα was examined by immunofluorescent labeling with specific

antibodies against BRG-1 and SRC-1. HeLa cells were transiently transfected with CFP-PR-A/B and YFP-ERα expression vectors, and then cultured in the presence or absence of E2 and P for 60 min before being stained with antibodies recognizing BRG-1 and SRC-1. Fluorescent images were captured using confocal laser scanning microscopy. The immunolabeling of BRG-1 and SRC-1 showed a discrete pattern in the nucleus being excluded from nucleolar regions, and was overlapped with the clusters of CFP-PR-A/B and YFP-ERα (Fig. 2).

Influence of Coexpression on the Mobility of ERα and PR-A/B

The colocalization of clusters of PR-A/B and ERα allowed us to speculate that their intranuclear mobilities affected each other. To examine this possibility, we carried out FRAP analysis. In the nucleus of COS-1 cells transfected with expression plasmids of YFP-PR-A, the YFP fluorescence of a randomly selected area (red circle; d = 0.5 μm) was photobleached, and then the images were captured at the indicated times after photobleaching. When FRAP analysis was performed with the cells that were not treated with P, we could not observe the bleached area, and this led to a reduction in the total nuclear fluorescence level (arrowhead, Fig. 3A). This indicates that the unliganded receptor is extremely mobile in the nucleus, and that a number of receptors passed through the bleach area, even during the time course of the bleaching. In the cells treated with P for 16 h, a clear dark area could be observed immediately after bleaching (0 s), but the fluorescence of the area was recovered and reached even with the neighboring clusters after 4.931 s (arrowhead, Fig. 3B). To evaluate the mobility of the receptors statistically, the time spent recovering half fluorescence (t1/2) was determined from the fluorescence intensity curve generated from 20 individual cells, and the mean was calculated to be 3.780 s (Fig. 4A).

The mobility of YFP-PR-B in the absence of ligand was also extremely high, comparable to that of YFP-ERα (data not shown). Ligand

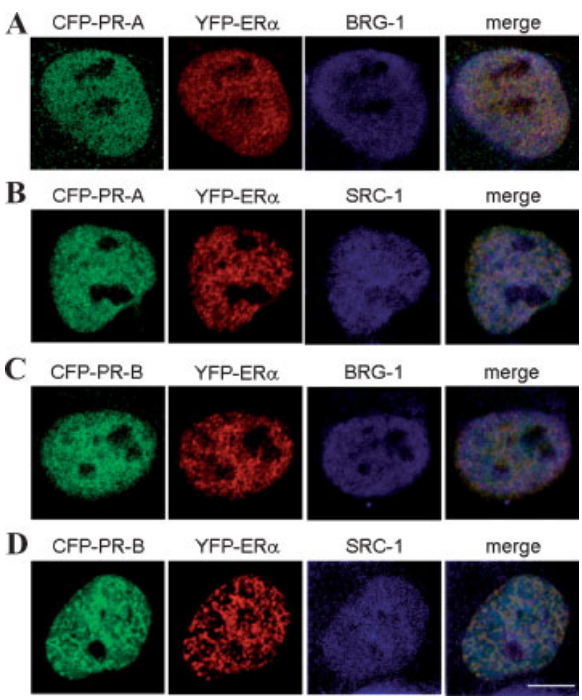

Fig. 2. Colocalization of BRG-1 and SRC-1 with the clusters of FP-PR-A/B and FP-ERα. HeLa cells transfected with the CFP-PR-A/B and YFP-ERα expression plasmids were cultured in the presence of E2 and P for 60 min. The cells were fixed and stained with anti-BRG-1 (**A**,**C**) or anti-SRC-1 (**B**,**D**). All images were captured using confocal laser scanning microscopy. Fluorescent images pseudocolored in green are distribution of CFP-PR-A (A,B) and CFP-PR-B (C,D). The images pseudocolored in red are distribution of YFP-ERα. The images pseudocolored in blue are distribution of BRG-1 (A,C) and SRC-1 (B,D). Merged images are shown in the right panels. Bar, 5μm.

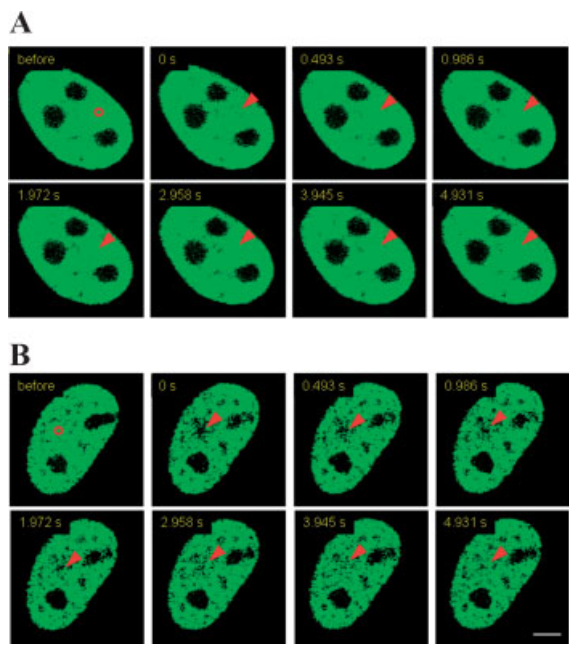

Fig. 3. FRAP analysis of PR-A. COS-1 cells were transfected with pYFP-PR-A. The fluorescence of YFP-PR-A in the indicated area (red circle; d = 0.5mm) within the nucleus of the cells treated (16–20 h) (**B**) and untreated (**A**) with ligand was bleached and the images were captured at the indicated times after bleaching. Arrow heads indicate the bleached position. Bar, 5μm.

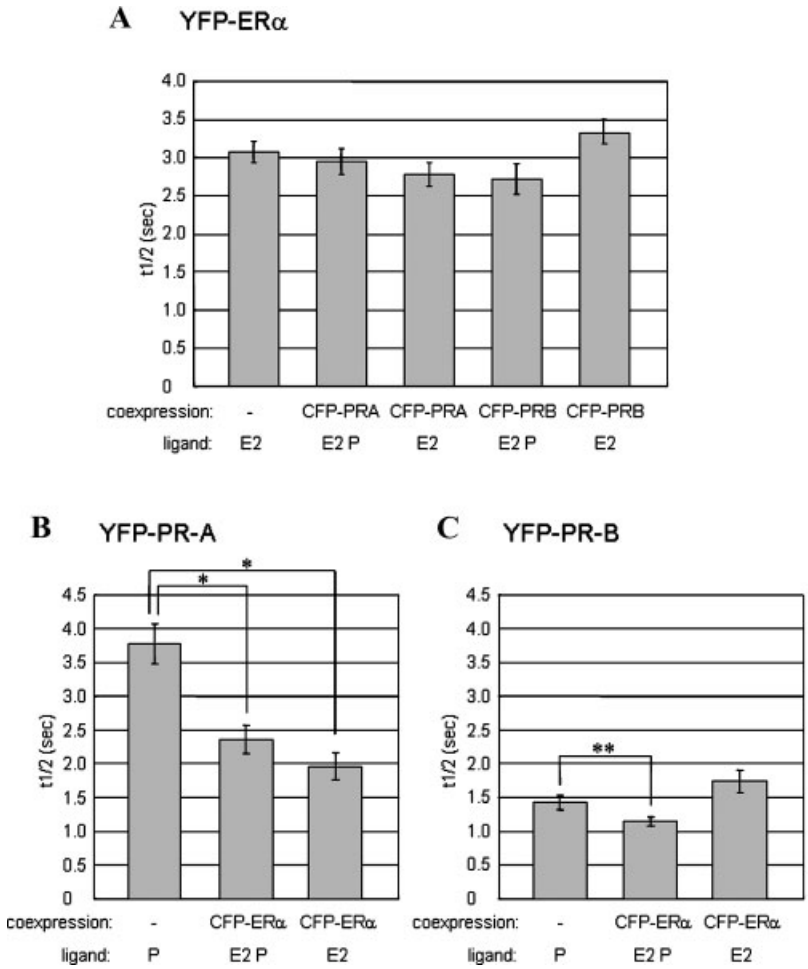

Fig. 4. Influence of coexpression on mobility of ERα and PR-A/B. COS-1 cells were cotransfected with the indicated expression plasmids and treated with E2 and/or P for 16–20 h. FRAP analysis of 20 independent cells in each experiment was performed and the t1/2 was measured. The data represents the mean ± SEM. **A**: Influence of the coexpression of PR-A or -B on the mobility of ERα. **B**: Influence of the coexpression of ERα on the mobility of PR-A. **C**: Influence of the coexpression of ERα on the mobility of PR-B. The values were significantly different at $*P < 0.03$ and $**P < 0.0003$ from Student's *t*-test.

activation slowed the recovery of YFP-PR-A/B, but their mobilities were still rapid. The mobility was higher in YFP-PR-B with a t1/2 of 1.426 s than in YFP-PR-A (Fig. 4B,C). We analyzed the mobility of YFP-ERα by coexpressing CFP-PR-A-or -B in the presence of both ligands, and there was no significant difference in the recovery of YFP-ERα in the case of transfection alone (Fig. 4A). In contrast, the recovery of ligand-activated YFP-PR-A and -B was hastened significantly by coexpressing ligand-activated CFP-ERα (Fig. 4B,C). These mobility changes of YFP-PR-A/B was depending on the coexpression of ERα, since, when YFP-PR-A/B were expressed singly, the mobility of YFP-PB-A/B was not changed by the addition of E2 (data not shown). There was a difference in the influence of the coexpression of ligand free CFP-ERα on the mobility of PR subtypes. The recovery of activated YFP-PR-A was hastened significantly, even in the presence of ligand free CFP-ERα (Fig. 4B), but that of YFP-PR-B was not (Fig. 4C).

Nuclear Matrix Binding Content of ERα and PR-A/B

Previous study reported that GFP-ERα bound to the nuclear matrix ligand-dependently with a similar time course to endogenous ERα. Most of the ligand-activated GFP-ERα remained within the nucleus by forming discrete clusters, even after the treatment of detergent and DNaseI;

whereas, unliganded GFP-ERα was present in the detergent-soluble fraction [Stenoien et al., 2000]. The YFP-ERα used in this study showed the same nuclear matrix binding property (Fig. 5a–e). YFP-PR-A and -B were also washed out after the detergent treatment in the absence of ligand (Fig. 5g,l). In the presence of ligand, the fluorescence of YFP-PR-A and -B still remained after the treatment of the detergent, but the fluorescence intensity was much weaker than that of YFP-ERα. The fluorescence intensities were not markedly changed by the treatment with DNaseI (Fig. 5i,j,n,o). These results suggest that YFP-PR-A and -B bind to the nuclear matrix ligand-dependently, but the proportion and/or strength of nuclear matrix binding of YFP-PR-A/B were lower than those of YFP-ERα.

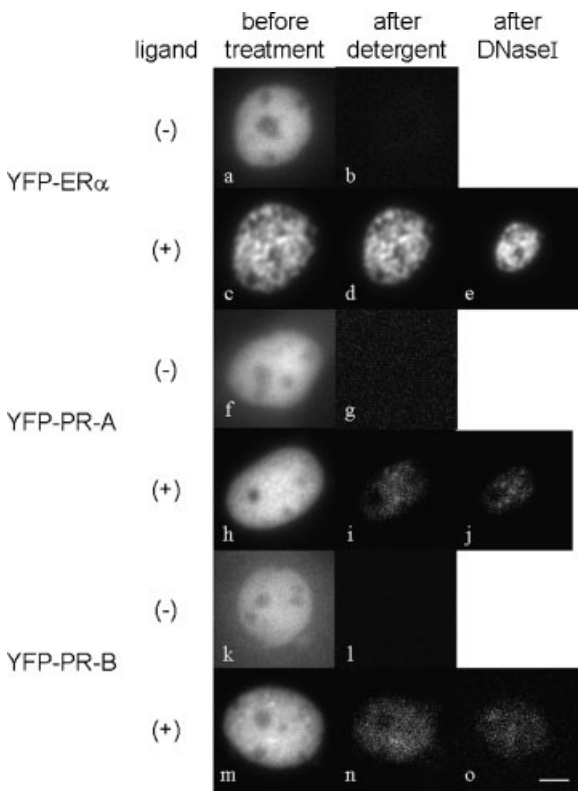

Fig. 5. Nuclear matrix binding analysis of ERα and PR-A/B. COS-1 cells were seeded on a glass base dish with a grid, transfected with the expression plasmid of YFP-ERα (**a**–**e**), PR-A (**f**–**j**), or PR-B (**k**–**o**), and treated with E2 (c,d,e) or P (h,i,j,m,n,o) for 1 h. Before permeabilization, fluorescent images were captured (a,c,f,h,k,m). After treating with a buffer containing 0.5% Triton X-100 for 3 min, fluorescent images of the same cells were captured (b,d,g,i,l,n). Then, the cells were treated with DNaseI, 0.25 M ammonium sulfate and 2 M NaCl, sequentially. Fluorescent images of the same cells were captured (e,j,o). Bar, 5μm.

The colocalization of FP-PR-A/B and FP-ERα in the clusters and the alteration of the mobility of liganded PR-A/B by ERα shown in this study suggest that the nuclear matrix binding amounts of the receptors were altered by the coexpression. Then, we examined nuclear matrix binding status of YFP-PR-A/B and CFP-ERα in the cells coexpressing both receptors and treated with both ligands (Fig. 6). However, we did not observe a significant difference in the nuclear matrix binding pattern from the case when YFP-PR-A, -B or YFP-ERα was singly transfected, meaning that the nuclear matrix binding contents of ERα and PR-A/B did not affect each other.

It has been reported that ATP-depletion resulted in nuclear matrix binding of unliganded ERα [Stenoien et al., 2000]. Thus, we examined the extent of nuclear matrix binding of YFP-PR-A/B as well as YFP-ERα in ATP-depleted cells (Fig. 7). Most of YFP-ERα was bound to the nuclear matrix at both unliganded and liganded states. Interestingly, most of YFP-PR-A/B was also bound to nuclear matrix at

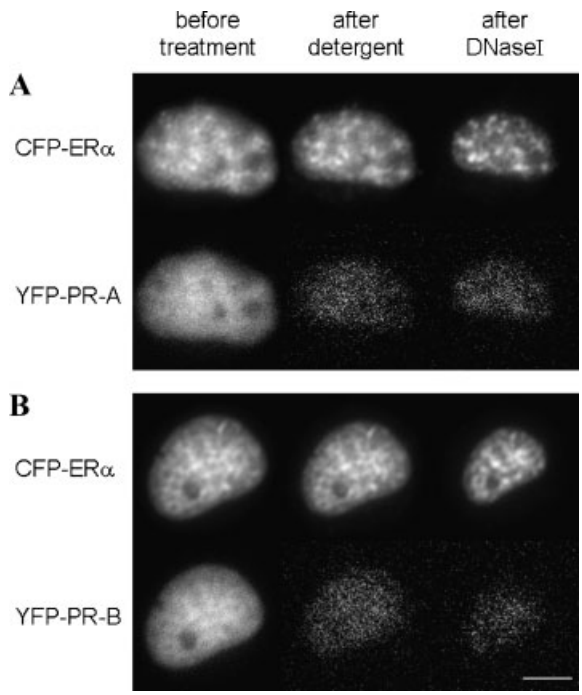

Fig. 6. Influence of coexpression on nuclear matrix binding of ERα and PR-A/B. COS-1 cells were cotransfected with the expression plasmids of CFP-ERα and YFP-PR-A (**A**) or CFP-ERα and YFP-PR-B (**B**) and treated with E2 and P. Nuclear matrix extraction was performed as in Fig. 5, and CFP (**upper**) and YFP (**lower**) fluorescent images in a cell were captured. Bar, 5μm.

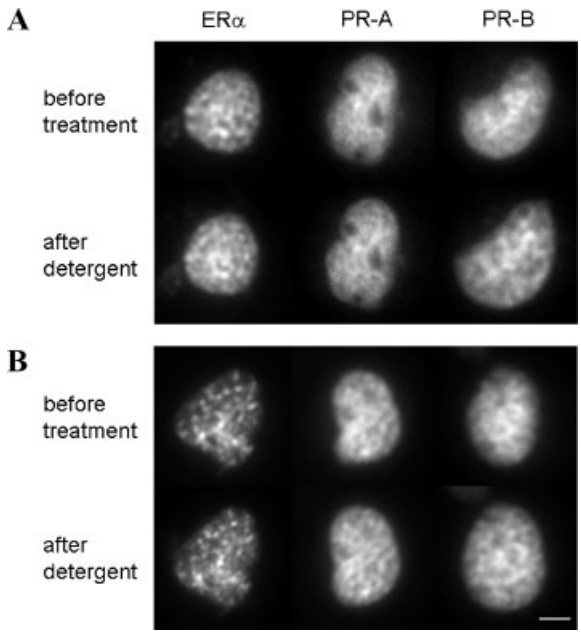

Fig. 7. Nuclear matrix binding of ERα and PR-A/B in ATP-depleted cells. COS-1 cells were transfected with the expression plasmid of YFP-ERα, YFP-PR-A, or YFP-PR-B. Before (**A**) or after (**B**) the treatment with E2 (for YFP-ERα) or P (for YFP-PR-A/B) for 4 h, culture medium was changed to ATP-depletion medium for 60 min. Before permeabilization, fluorescent images were captured (before treatment). After treating with a buffer containing 0.5% Triton X-100 for 3 min, fluorescent images of the same cells were captured (after detergent). Bar, 5μm.

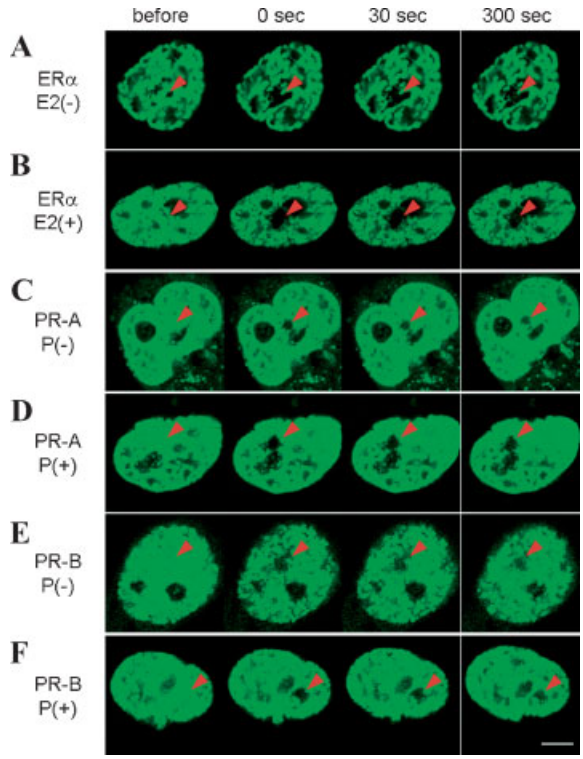

Fig. 8. Loss of mobility of ERα and PR-A/B in ATP-depleted cells. COS-1 cells were transfected with pYFP-ERα (**A**,**B**), pYFP-PR-A (**C**,**D**), or pYFP-PR-B (**E**,**F**). Fluorescence of the indicated area (d = 0.5mm) within the nucleus of the cells treated (4 h) (B,D,F) and untreated (A,C,E) with ligand was bleached and the images were captured at the indicated times after bleaching. Arrow heads indicate the bleached position. Bar, 5μm.

both states showing a highly discrete distribution pattern, regardless of their low binding capacity in the presence of ATP.

ATP-Depletion Extinguishes the Mobility of ERα and PR-A/B Both in the Absence and Presence of Ligand

Intensive nuclear matrix binding of ERα and PR-A/B in ATP-depleted cells indicates the reduction of the mobility of the receptors. It was reported that the immobilization of ERα in living ATP-depleted cells occurred in the absence of ligand, but not in the presence of ligand [Stenoien et al., 2000]. However, in the present study, we observed the immobilization of YFP-ERα both in ligand-untreated and -treated cells, because the fluorescence of the bleached area was not recovered after 300 s (arrow head, Fig. 8A,B). We think that the difference between the previous and present study in the liganded ERα mobility is due to the difference of incubation time in the ATP-depletion medium. We cultured the cells in ATP-depletion medium for a longer time (60 min) than the previous study (15 min) according to the report, which measured the intracellular ATP concentration [Tang and DeFranco, 1996]. Elbi et al. [2004] demonstrated that ATP was necessary for the nuclear mobility of PR using permeabilized and extracted cells. We verified the ATP-dependency of the PR mobility in living cells. In the ATP-depleted cells, PR-A/B were immobilized within the nucleus, both in the absence and presence of ligand (Fig. 8C–F).

Colocalization of ERα and PR-A/B With NuMA

NuMA is a principal component protein of the nuclear matrix in interphase cells [Zeng et al., 1994; Harborth et al., 1999; Gribbon et al., 2002] and was shown to be colocalized with glucocorticoid receptor (GR) in ATP-depleted cells by immunofluorescence study [Elbi et al., 2004]. To examine the colocalization of ERα and PR-A/B with NuMA in living cells, we cotransfected the expression plasmids of CFP-ERα or

CFP-PR-A/B and NuMA-YFP. As shown in the previous reports [Elbi et al., 2004; Kisurina-Evgenieva et al., 2004], NuMA-YFP distributed non-uniformly throughout the nucleus, except for the nucleoli (Fig. 9A). Ligand-activated CFP-ERα and CFP-PR-A/B were colocalized with NuMA-YFP, but clusters of the receptors and the area where NuMA-YFP was highly accumulated was separately distributed with in the nucleus.

ATP-Dependent Dynamics of NuMA

Although the molecular dynamics of NuMA in mitotic phase were clearly demonstrated [Kisurina-Evgenieva et al., 2004], those of interphase have not been shown. If this nuclear matrix component protein was exchanged rapidly, the possibility that the mobility of liganded ERα and PR-A/B was due to the nuclear matrix dynamics could be considered. Therefore, we examined the mobility of NuMA-GFP in the interphase nucleus with FRAP analysis. In a cell expressing NuMA-GFP construct, a dark area was observed immediately after bleaching (0 s). Then, the fluorescence of the area was recovered rapidly (t1/2 = 30.8 s) and reached a level similar to the surrounding area after 240 s (arrowhead, Fig. 9B upper). This result indicates that the nuclear matrix itself is dynamic in interphase nucleus, while the mobility of the nuclear matrix is lower than the mobility of ERα and PR-A/B. We next examined the ATP-dependency of the NuMA dynamics. In ATP-depleted cells, the fluorescence recovery was hardly detectable in the bleached area over 240 s (arrowhead, Fig. 9B middle). This phenomenon suggests a strong correlation between nuclear matrix dynamics and the mobility of ERα and PR-A/B, since, as shown in Fig. 8, mobility of the receptors also depends on ATP. However, the involvement of proteasome, which was known as another mechanism regulating the mobility of ERα, in

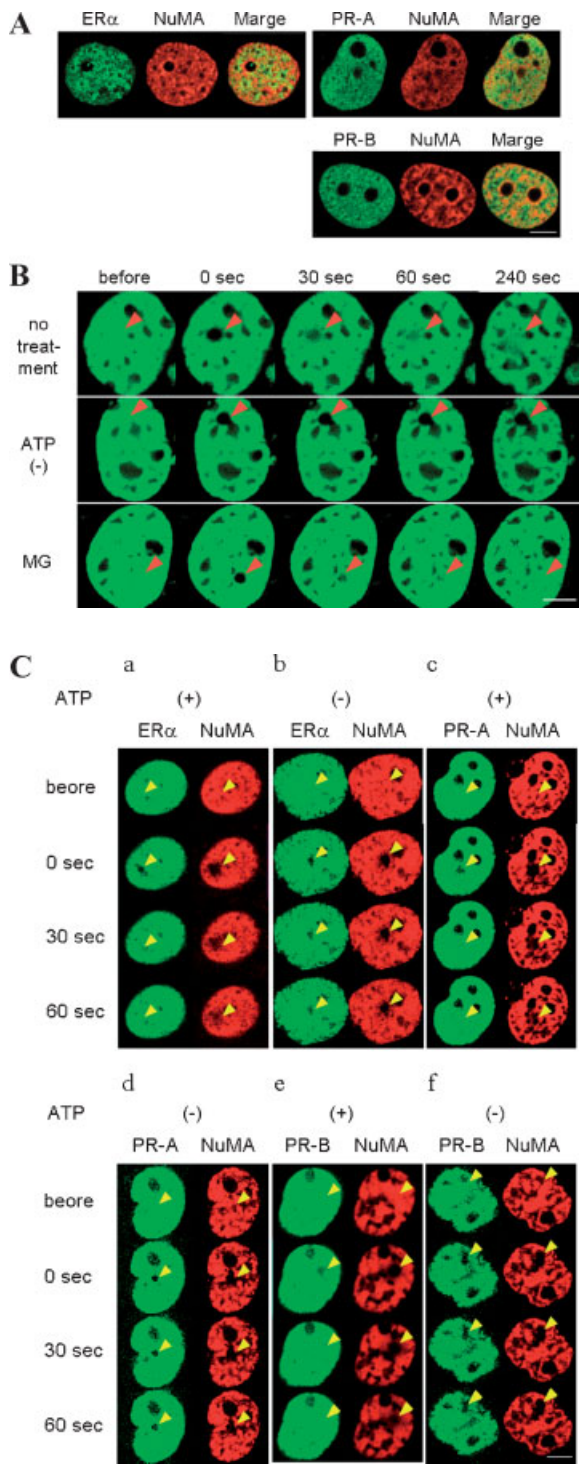

Fig. 9. Colocalization with ERα and PR-A/B and the dynamics of NuMA. **A**: COS-1 cells were cotransfected with pNuMA-YFP and pCFP-ERα, pCFP-PR-A, or pCFP-PR-B and treated with ligand for 4 h. Fluorescence image of CFP and YFP was captured and pseudocolored green and red, respectively. Merged image is shown in the **right panels**. **B**: COS-1 cells were transfected with pNuMA-GFP. The fluorescence of the indicated area (d = 0.5mm) within the nucleus of the cells untreated (**upper**), cultured in ATP-depletion medium for 60 min (**middle**) and treated with MG132 for 5 h (**lower**) was bleached and the images were captured at the indicated times after bleaching. Arrow heads indicate the bleached position. **C**: COS-1 cells were cotransfected with pNuMA-YFP and pCFP-ERα (**a**,**b**), pCFP-PR-A (**c**,**d**), or pCFP-PR-B (**e**,**f**) and treated with ligand for 4 h. Fluorescence of the indicated area (d = 0.5mm) within the nucleus of the cells untreated (a,c,d) and cultured in ATP-depletion medium for 60 min (b,d,f) was bleached, and the images were captured at the indicated times after bleaching and pseudocolored green and red, respectively. Arrow heads indicate the bleached position. Bar, 5μm.

NuMA dynamics was not observed. In the cells treated with a proteasome inhibitor, MG132, the fluorescence of the bleached area (arrowhead, Fig. 9B lower) was recovered with a similar time course (t1/2 = 29.3 s) to non-treated cells. In the cells coexpressing NuMA-YFP and CFP-ERα or CFP-PR-A/B, the fluorescence recovery of CFP-ERα or CFP-PR-A/B was observed in the bleached area prior to the fluorescence recovery of NuMA-YFP (arrowhead, Fig. 9C (a,c,e)), while the recovery of both fluorescences was not detectable in ATP-depleted cells (arrow head, Fig. 9C (b,d,f)).

DISCUSSION

It is known that GFP-ERα and ERβ redistribute from a diffuse to discrete pattern in response to the ligand [Htun et al., 1999; Stenoien et al., 2000; Matsuda et al., 2002]. Deletion analysis suggested that discrete cluster formation of ERs did not occur, irrespective of the receptor function [Matsuda et al., 2002]. The discrete clusters of ERα and ERβ are associated with SRC-1 and a chromatin remodeling protein, BRG-1; therefore, ERs clusters are believed to be involved in the transcriptional regulation through structural changes of chromatin. As shown in this study, FP-PR-A and -B also exhibited ligand-dependent non-uniform distribution within the nucleus, but the degree of cluster formation was lower than that of ERs. The nuclear areas where PR-A/B was relatively accumulated were colocalized with clusters of ERα, SRC-1, and BRG-1, suggesting that PR-A/B and ERα shared or competed with such coregulator molecules at the clusters. A number of reports demonstrated that ERα and PR-A/B had synergistic or inhibitory cross-talk in their transcriptional regulation [Cato and Ponta, 1989; Meyer et al., 1989; Wen et al., 1994; Kraus et al., 1995]. The sharing or competition of coregulator molecules, therefore, may be involved in the cross-talk of ERα and PR-A/B. While intranuclear interaction between ERβ and PR-A/B has not been reported, cluster formation and colocalization with SRC-1 and BRG-1 indicate that ERβ may also exhibit cross-talk with PR-A/B through the sharing or competition of coregulator molecules.

Colocalization of FP-PR-A/B and FP-ERα indicates that their intranuclear mobilities affected each other. It is well known that steroid hormone receptors are dynamically mobile exhibiting second order recovery by FRAP analysis in the nucleus, as well as on the biding site of the promoter [McNally et al., 2000; Stenoien et al., 2001; Ochiai et al., 2004]. The mobility of FP-PR-A/B shown in this study was also dynamic; thus, the high mobility within the nucleus may be a common characteristic of ligand-activated steroid hormone receptors. The mobility of FP-PR-A/B was increased by the coexpression of FP-ERα; whereas, the mobility of FP-ERα was not changed by the coexpression of FP-PR-A/B. We have reported that the mobility of FP-AR was also increased by the coexpression of FP-ERα [Ochiai et al., 2004], indicating that ERα might influence the transcriptional activity of other sex steroid hormone receptors by changing the mobility of the receptors. If so, it is important to solve the mechanism of ERα to influence the mobility of PR-A/B and AR. Factors responsible for the intranuclear mobility of steroid hormone receptors are being identified. Elbi et al. [2004] demonstrated that the nuclear mobility of GR was inhibited by geldanamycin, which blocks the chaperone activity of heat-shock protein 90, and that multiple chaperone/cochaperone complexes possessed the ability to function as a nuclear mobility factor for GR and PR. Stenoien et al. [2001] reported that the treatment with a proteasome inhibitor, MG132, caused ERα to stay at the same nuclear position for longer time due to the tight association with the nuclear matrix. In addition, Stavreva et al. [2004] demonstrated that the rapid exchange of GR at the transcriptionally on-going promoter was regulated by chaperones and proteasomes. According to these findings, we speculated that the increase of mobility of FP-PR-A/B and FP-AR by FP-ERα was due to competition for binding with chaperone/cochaperone proteins and proteasomes and/or a change of molecular balance of chaperone/cochaperone proteins that bind with FP-PR-A/B and FP-AR.

It was reported previously that most of the ligand-activated ERα was associated with the nuclear matrix by forming the discrete clusters [Barrack, 1987; Stenoien et al., 2000]. PR-A/B also exhibited nuclear matrix binding capacities, but the rate of the receptor that was associated with the nuclear matrix was lower than that of ERα. This phenomenon coincided with the degree of cluster formation of ERα and PR-A/B, suggesting that cluster formation and nuclear matrix binding were correlated

with each other. Colocalization of ERα and PR-A/B indicates competition for nuclear matrix molecules. However, the nuclear matrix binding contents of ligand-activated ERα and PR-A/B did not affect each other. Upon the addition of ligand, most of the ERα bound to the nuclear matrix by forming clusters, while a lesser amount of PR-A/B bound with the nuclear matrix. ATP-depletion led PR-A/B as well as ERα to tightly associate with nuclear matrix in the presence of ligand, regardless of the lower binding efficiency of PR-A/B in the presence of ATP. The diffuse nuclear distributions of ERα and PR-A/B in the absence of ligand allowed us to hypothesize that these receptors move freely by Brownian diffusion within the nucleus; however, the tight association of ERα and PR-A/B with the nuclear matrix caused by ATP-depletion was also observed in the unliganded state. In addition, the intranuclear mobility of ERα and PR-A/B was extinguished by ATP-depletion. These results indicate that there may be unknown ATP-dependent mechanisms that regulate rate, length, and/or strength of nuclear matrix binding of the ovarian steroid hormone receptors to maintain their abilities as transcriptional factors, and that the sensitivity to these mechanisms may be different between ERα and PR-A/B.

As the molecular basis for the nuclear mobility of ERα and PR-A/B in association with nuclear matrix binding, two models could be considered; one was repetition of the process of attaching to and detaching from the stable nuclear matrix, and the other was tight binding to the unstable nuclear matrix. To elucidate which model was taking place in the cells, the stability of the nuclear matrix was examined by analyzing the mobility of NuMA-FP. NuMA-FP was distributed non-uniformly within the nucleus, and colocalized with the clusters of FP-ERα and FP-PR-A/B in the region where NuMA-FP was less densely accumulated, indicating that NuMA was involved in the transcriptional regulations in this region [Zeng et al., 1994; Gribbon et al., 2002]. The rapid recovery of the fluorescence of NuMA-FP after photobleaching suggests that the nuclear matrix is also reconstructed continuously in the nucleus. Therefore, it could be considered that the mobility of the ligand-activated ERα and PR-A/B was at least partially due to the dynamics of nuclear matrix. The replacement of the NuMA molecule, however, was slower than the mobility of ERα and PR-A/B, suggesting that the mobility of the receptors not only depended on the nuclear matrix dynamics, but also on the temporal binding to the nuclear matrix. When the involvement of ATP and the proteasome, which are known to regulate the mobility of the receptors [Stenoien et al., 2001; Elbi et al., 2004], in NuMA dynamics was investigated, ATP-depletion blocked the replacement of NuMA, but the inhibition of proteasome activity did not. According to these findings, we propose the possibility that in the mobility of ERα and PR-A/B in association with nuclear matrix binding, ATP was related to the nuclear matrix dynamics, and the proteasome activity was related to the binding of the receptors with the nuclear matrix. Tight association of ERα and PR-A/B to the nuclear matrix in ATP-depleted cells may be due to the elimination of the nuclear matrix plasticity. The elucidation of detailed mechanisms of these processes may greatly progress our understanding of the molecular properties of the ovarian steroid hormone receptors.

ACKNOWLEDGMENTS

The authors thank Dr. B. Katzenellenbogen, Dr. D. A. Compton and Dr. T. Inoue for providing plasmids. We thank I. Ochiai, Y. Kurihara, H. Fukuoka, K. Kimura, M. Kataoka, H. Tada, E. Ishida, and A. Takara for their technical assistance.

REFERENCES

Barrack ER. 1987. Steroid hormone receptor localization in the nuclear matrix: Interaction with acceptor sites. J Steroid Biochem 27:115–121.

Cato AC, Ponta H. 1989. Different regions of the estrogen receptor are required for synergistic action with the glucocorticoid and progesterone receptors. Mol Cell Biol 9:5324–5330.

Cowley SM, Hoare S, Mosselman S, Parker MG. 1997. Estrogen receptors α and β form heterodimers on DNA. J Biol Chem 272:19858–19862.

Elbi C, Walker DA, Romero G, Sullivan WP, Toft DO, Hager GL, DeFranco DB. 2004. Molecular chaperones function as steroid receptor nuclear mobility factors. Proc Natl Acad Sci USA 101:2876–2881.

Giangrande PH, Kimbrel EA, Edwards DP, McDonnell DP. 2000. The opposing transcriptional activities of the two isoforms of the human progesterone receptor are due to differential cofactor binding. Mol Cell Biol 20:3102–3115.

Greco B, Allegretto EA, Tetel MJ, Blaustein JD. 2001. Coexpression of ER β with ER α and progestin receptor proteins in the female rat forebrain: Effects of estradiol treatment. Endocrinology 142:5172–5181.

Greene GL, Gilna P, Waterfield M, Baker A, Hort Y, Shine J. 1986. Sequence and expression of human estrogen receptor complementary DNA. Science 231:1150–1154.

Gribbon C, Dahm R, Prescott AR, Quinlan RA. 2002. Association of the nuclear matrix component NuMA with the Cajal body and nuclear speckle compartments during transitions in transcriptional activity in lens cell differentiation. Eur J Cell Biol 81:557–566.

Harborth J, Wang J, Gueth-Hallonet C, Weber K, Osborn M. 1999. Self assembly of NuMA: Multiarm oligomers as structural units of a nuclear lattice. EMBO J 18:1689–1700.

Hora J, Horton MJ, Toft DO, Spelsberg TC. 1986. Nuclease resistance and the enrichment of native nuclear acceptor sites for the avian oviduct progesterone receptor. Proc Natl Acad Sci USA 83:8839–8843.

Htun H, Holth LT, Walker D, Davie JR, Hager GL. 1999. Direct visualization of the human estrogen receptor α reveals a role for ligand in the nuclear distribution of the receptor. Mol Biol Cell 10:471–486.

Hu LM, Bodwell J, Hu JM, Orti E, Munck A. 1994. Glucocorticoid receptors in ATP-depleted cells. Dephosphorylation, loss of hormone binding, HSP90 dissociation, and ATP-dependent cycling. J Biol Chem 269:6571–6577.

Inoue T, Kamiyama J, Sakai T. 1999. Sp1 and NF-Y synergistically mediate the effect of vitamin D(3) in the p27(Kip1) gene promoter that lacks vitamin D response elements. J Biol Chem 274:32309–32317.

Jarvinen TA, Pelto-Huikko M, Holli K, Isola J. 2000. Estrogen receptor β is coexpressed with ERα and PR and associated with nodal status, grade, and proliferation rate in breast cancer. Am J Pathol 156:29–35.

Kastner P, Krust A, Turcotte B, Stropp U, Tora L, Gronemeyer H, Chambon P. 1990. Two distinct estrogen-regulated promoters generate transcripts encoding the two functionally different human progesterone receptor forms A and B. EMBO J 9:1603–1614.

Kawata M, Yuri K, Ozawa H, Nishi M, Ito T, Hu Z, Lu H, Yoshida M. 1998. Steroid hormones and their receptors in the brain. J Steroid Biochem Mol Biol 65:273–280.

Kawata M, Matsuda K, Nishi M, Ogawa H, Ochiai I. 2001. Intracellular dynamics of steroid hormone receptor. Neurosci Res 40:197–203.

Kisurina-Evgenieva O, Mack G, Du Q, Macara I, Khodjakov A, Compton DA. 2004. Multiple mechanisms regulate NuMA dynamics at spindle poles. J Cell Sci 117:6391–6400.

Kraus WL, Weis KE, Katzenellenbogen BS. 1995. Inhibitory cross-talk between steroid hormone receptors: Differential targeting of estrogen receptor in the repression of its transcriptional activity by agonist- and antagonist-occupied progestin receptors. Mol Cell Biol 15:1847–1857.

Kuiper GG, Enmark E, Pelto-Huikko M, Nilsson S, Gustafsson JA. 1996. Cloning of a novel receptor expressed in rat prostate and ovary. Proc Natl Acad Sci USA 93:5925–5930.

Lau KM, Mok SC, Ho SM. 1999. Expression of human estrogen receptor-α and -β, progesterone receptor, and androgen receptor mRNA in normal and malignant ovarian epithelial cells. Proc Natl Acad Sci USA 96:5722–5727.

Lim CS, Baumann CT, Htun H, Xian W, Irie M, Smith CL, Hager GL. 1999. Differential localization and activity of the A- and B-forms of the human progesterone receptor using green fluorescent protein chimeras. Mol Endocrinol 13:366–375.

Matsuda K, Ochiai I, Nishi M, Kawata M. 2002. Colocalization and ligand-dependent discrete distribution of the estrogen receptor (ER)α and ERβ. Mol Endocrinol 16: 2215–2230.

McNally JG, Muller WG, Walker D, Wolford R, Hager GL. 2000. The glucocorticoid receptor: Rapid exchange with regulatory sites in living cells. Science 287:1262–1265.

Meyer ME, Gronemeyer H, Turcotte B, Bocquel MT, Tasset D, Chambon P. 1989. Steroid hormone receptors compete for factors that mediate their enhancer function. Cell 57: 433–442.

Nishi M, Tanaka M, Matsuda K, Sunaguchi M, Kawata M. 2004. Visualization of glucocorticoid receptor and mineralocorticoid receptor interactions in living cells with GFP-based fluorescence resonance energy transfer. J Neurosci 24:4918–4927.

Ochiai I, Matsuda K, Nishi M, Ozawa H, Kawata M. 2004. Imaging analysis of subcellular correlation of androgen receptor and estrogen receptor α in single living cells using green fluorescent protein color variants. Mol Endocrinol 18:26–42.

Ogawa H, Inouye S, Tsuji FI, Yasuda K, Umesono K. 1995. Localization, trafficking, and temperature-dependence of the Aequorea green fluorescent protein in cultured vertebrate cells. Proc Natl Acad Sci USA 92:11899–11903.

Pace P, Taylor J, Suntharalingam S, Coombes RC, Ali S. 1997. Human estrogen receptor β binds DNA in a manner similar to and dimerizes with estrogen receptor α. J Biol Chem 272:25832–25838.

Richer JK, Jacobsen BM, Manning NG, Abel MG, Wolf DM, Horwitz KB. 2002. Differential gene regulation by the two progesterone receptor isoforms in human breast cancer cells. J Biol Chem 277:5209–5218.

Stavreva DA, Muller WG, Hager GL, Smith CL, McNally JG. 2004. Rapid glucocorticoid receptor exchange at a promoter is coupled to transcription and regulated by chaperones and proteasomes. Mol Cell Biol 24:2682–2697.

Stenoien DL, Mancini MG, Patel K, Allegretto EA, Smith CL, Mancini MA. 2000. Subnuclear trafficking of estrogen receptor-α and steroid receptor coactivator-1. Mol Endocrinol 14:518–534.

Stenoien DL, Patel K, Mancini MG, Dutertre M, Smith CL, O'Malley BW, Mancini MA. 2001. FRAP reveals that mobility of oestrogen receptor-α is ligand- and proteasome-dependent. Nat Cell Biol 3:15–23.

Tang Y, DeFranco DB. 1996. ATP-dependent release of glucocorticoid receptors from the nuclear matrix. Mol Cell Biol 16:1989–2001.

Vegeto E, Shahbaz MM, Wen DX, Goldman ME, O'Malley BW, McDonnell DP. 1993. Human progesterone receptor A form is a cell- and promoter-specific repressor of human progesterone receptor B function. Mol Endocrinol 7: 1244–1255.

Wen DX, Xu YF, Mais DE, Goldman ME, McDonnell DP. 1994. The A and B isoforms of the human progesterone receptor operate through distinct signaling pathways within target cells. Mol Cell Biol 14:8356–8364.

Zeng C, He D, Berget SM, Brinkley BR. 1994. Nuclear-mitotic apparatus protein: A structural protein interface between the nucleoskeleton and RNA splicing. Proc Natl Acad Sci USA 91:1505–1509.